A Bi-Objective Optimization Model for Urban Rail Transit Train Timetable under Uncertain Passenger Demand

Runyu Wu, Cunjie Dai, Songlin Tian, Xiaoquan Wang, Tingyu Wang

***Abstract*—This paper proposes a method for optimizing the Urban Rail Transit train timetable, that minimizes the total passenger waiting time and the total train operation cost by scheduling two types of trains with different capacities after considering the uncertain passenger demand in both directions of the Urban Rail Transit line. Combining the constraints of various types of train operation safety and passenger carrying tasks, we establish a mixed integer nonlinear programming model and improve the multi-objective heuristic algorithm to obtain the corresponding solutions. Finally, numerical example is constructed based on the Xi'an Metro Line 2 data to verify the effectiveness of proposed method.**

***Index Terms*—Train Timetable, Uncertain Passenger Demand, Multi-objective, Heuristic Algorithm**

I. Introduction

To further improve the public's travel efficiency, many cities have solved the problem of urban traffic congestion by constructing Urban Rail Transit (URT) lines [1]. URT has played an essential role in the public transportation system of many large cities. However, due to various URT operators' different management and operation levels, the scientific nature of the train timetable developed by some URT lines is complex to guarantee. The phenomenon of insufficient or redundant capacity often occurs in its operational organization [1], which reduces the passengers' travel experience or the operating company's waste of investment.

Therefore, we will discuss this problem in this study, that is, under the premise of ensuring the operational safety of URT system, from the perspective of passengers and companies, comprehensively consider and then create a model and design an algorithm to solve it. Ultimately, we will get a highly efficient and scientific train timetable.

The train schedule can visually reflect the train's operation information in the time and space dimensions, which contains several aspects [2], such as the train's stopping time, arrival time, and departure time at each station. After B. Szpigel et al. [3] studied the optimization of train schedules of a single-line railroad to minimize the total travel time, many scholars and engineers conducted in-depth studies on optimizing train departure timetables under the rail transit system. C. Liebchen [4]portrayed the train schedules of the Berlin subway using a periodic event scheduling model and solved the problem to obtain the results of the reduction of passenger travel time and saving the number of trains; L. Kroon L et al. [5] used a stochastic optimization model to improve the robustness of train timetables, and then used the cost of rolling stock usage and staffing costs as resource constraints to design a more profitable train schedule for the Dutch Railways [6]. B. R. Ke et al. [7] used a two-phase algorithm to solve inter- and intra-station conflicts for a single-line freight train schedule optimization; E. Barrena et al. [8] used a branch-and-bound algorithm to compute train timetables for multiple problem scenarios and achieved better results than conventional timetables.

Combined with the passenger flow demand law to draw the train schedule, it can improve the coupling of trains and passenger flow demand. In the daily operating hours of URT lines, the number of passengers arriving at each station in different periods has a significant difference [9], which forms the phenomenon of the imbalance of URT passenger flow demand in time and space. The description of passenger demand in rail transit system is divided into two types: the first type is the use of mathematical theories and methods to study the distribution characteristics of rail transit passenger demand, L. X. Yang et al. [10] used triangular fuzzy vectors to portray the number of people boarding and alighting at each station along the train line; B. Serkan et al. [11] ,J. Liu et al. [12] used the dynamic passenger demand as a condition to optimize the train timetable; L. Meng et al. [13] developed a mixed-integer linear model to solve the train schedule and resource allocation plan by considering the dynamic choice behavior of passengers and their response to the train departure intervals; C. Gong et al. [14] found that the deterministic passenger flow is prone to the disadvantage of falling into a local optimal solution when solving the train schedule and speed profiles, and proved that a robust

Manuscript received July 29, 2024; revised November 24, 2024.

This research was supported by Natural Science Foundation of Gansu Province(23JRRA858), Science and Technology Program (Joint Research Fund) Project of Gansu Province(24JRRA868), Gansu Provincial Department of Education: Outstanding Graduate Students “Innovation Star” Program (2025CXZX-704).

Runyu Wu is a postgraduate student at the School of Traffic and Transportation, Lanzhou Jiaotong University, Lanzhou 730070, China. (e-mail: wurunyu001@163.com).

Cunjie Dai is an associate professor at the School of Traffic and Transportation, Lanzhou Jiaotong University, and Plateau Railway Transportation Intelligent Management and Control Railroad Industry Key Laboratory, Lanzhou 730070, China. (Corresponding author, phone: +86 13919467628, e-mail: daicunjie@mail.lzjtu.cn).

Songlin Tian is a postgraduate student at the School of Traffic and Transportation, Lanzhou Jiaotong University, Lanzhou 730070, China. (e-mail: lzjtuwxq@163.com).

Xiaoquan Wang is a postgraduate student at Dept of Xinjiang Railway Survey and Design Institute of China Railway First Institute, Comprehensive Design Sub-division, Urumqi 830000, China. (e-mail: lzjtuwxq@163.com).

Tingyu Wang is a postgraduate student at the School of Traffic and Transportation, Lanzhou Jiaotong University, Lanzhou 730070, China. (e-mail: 17855825504@163.com).

optimization method with a stochastic dynamic demand can avoid this disadvantage through a solver example. Powerful optimization methods can effectively prevent this problem.

The second type of representation of passenger demand in rail transit systems is time-varying demand, i.e., it is described using passenger trip origins and destinations (i.e., OD pairs). H. Niu et al. [15] developed a nonlinear optimization model by combining the passenger boarding and departure events for a detailed description of oversaturated passenger flow during peak hours. Then, they designed a generalized quadratic programming integer model for a given train hopping pattern [16]. Similarly, many researchers and technicians have directly used passenger OD to represent passenger demand ([17]-[20]).

Although the primary task of URT systems is to serve passengers, it is also imperative for the operating companies to utilize their resources rationally to reduce the corresponding cost investment [21]. Therefore, it is worthwhile to consider the development of train timetables from the perspectives of passengers and operators ([22]-[24]), which has been proved by D. Canca et al. [25], in the time-varying characteristics of the passenger demand, the URT operators use a fixed departure interval mode of transportation organization, which will make part of the passengers on the URT line waiting time at the station is too long. is too long.

With time, the related research based on this point of view has been deepened and expanded. J. E Cury et al. [26] improved the train schedule by analyzing the passenger flow demand of the north and south lines of the Sao Paulo metro company in Brazil and combining the existing resource allocation of the metro company. Based on bi-level programming, T. Albrecht [27] designed the optimal train timetable for a suburban railway after calculating the passenger demand and train capacity. H. J. Sun et al. [28] proposed a bi-objective optimization model to optimize the total waiting time of passengers and the energy consumption of train operations. The train timetable optimization model established by X. Yang et al. [29] considers improving the utilization of renewable energy while shortening the waiting time of passengers. P. Mo et al. [30] felt the imbalance of passenger flow demand. They optimized the train operation plan with the intention of minimizing the energy cost of train operation and passenger waiting time. In addition, due to the similarity of operation mode between URT and high-speed railway [31], many optimization theories and methods for high-speed railway train operation plans can provide a reference for our research.

After we summarize the research content of the related literature, we can intuitively find that the established rail transit system train timetables have the following characteristics: (1) the existing literature mostly considers trains of a single formation type, and there is little literature that considers scheduling multiple formation types of trains when compiling the URT train timetables; (2) the existing literature mostly expresses the passenger demand as the total station-to-station and time-varying demand, and there are fewer related researches that portray the passenger flow demand as an uncertain variable.

Compared with the established literature, our study provides the following innovations to the increasingly mature research work on URT train timetables:

(1) In this paper, the formation type of operating trains is used as a decision variable, and two types of trains with different capacities are dispatched in the preparation of train timetables.

(2) To reflect the stochastic nature of passenger demand, the number of people boarding and alighting from each train is portrayed using chance programming method.

(3) A two-objective optimization model is established, and the variational operation of the NSGA-II algorithm is improved using an adaptive large-scale neighborhood search strategy for the solution.

The content of this study is set up in the following order. Section 2 presents a detailed description of the considered problem, passenger flow demand, and multiple-unit train operation mode. In Section 3, we establish a bi-objective optimization model for train timetables to ensure the safety of train operation and accomplish the passenger flow demand. Section 4 describes an improved algorithm based on NSGA-II with a variational strategy designed to improve the quality and speed of the solution. The results of numerical experiments are compared and analyzed in Section 5 to demonstrate the performance of the proposed method. Finally, this study concludes and discusses future research directions.

II. Problem Statement and Theoretical Basis

A. Problem statement

This article aims to design train timetables on a bi-directional URT line. To facilitate the portrayal of passengers' travel directions and improve the convenience of calculation, we divide a station into two stations in both operation directions as shown in Fig. 1. In detail, Station 1 to Station $|N|$ is the upstream direction and Station $|N|+1$ to Station $2|N|$ is the downstream direction. When there is no situation affecting the train operation, the stopping time of the train at each station is fixed.

In this paper, our study focuses on the service area, in other words, we do not consider the articulation sequence of trains in the circulation area, and only improve its match with passenger demand by optimizing the sequence of trains in the service area.

B. Passenger demand analysis

Taking the departure passenger demand of the station u on the URT line as an example, when the station $u, v \in \{1, 2, \cdots, |N|\}$ and the number $u<v$ define the passenger demand density is $\varsigma_{u,v}(t)$ from station u to station v on the timestamp t.

Stipulate $\varsigma_{u,v}(t) = 0$ when $u \in \{1, 2, \cdots, |N|\}$ and $v \in \{|N|+1, |N|+2, \cdots 2|N|\}$. In Fig. 2(a), the blue solid line represents $\varsigma_{u,v}(t)$, and the red dashed line represents $\psi_{u,v}(t)$. $\psi_{u,v}(t)$ is passenger demand from station u to station v in the range of timestamp 0 to timestamp t, and its calculation method is shown in Equation (1):

$$\psi_{u,v}(t) = \int_0^t \varsigma_{u,v}(t)\ \mathrm{d}t,\ u, v \in \{1, 2, \cdots, |N|\} \tag{1}$$

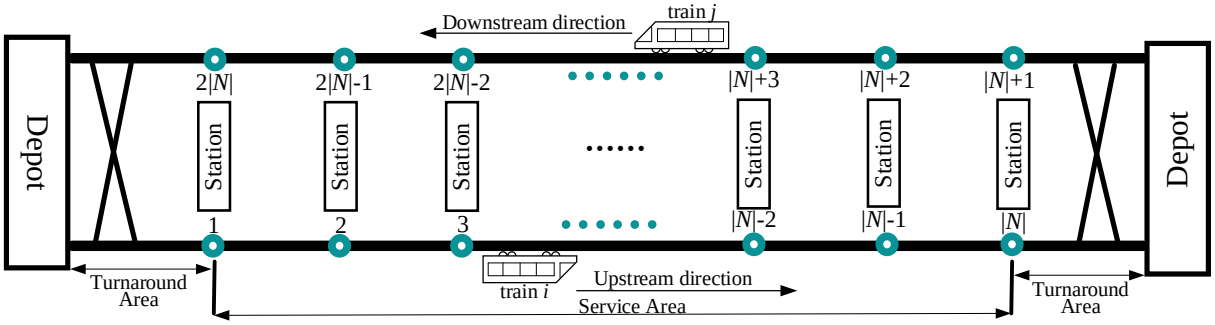

Fig. 1 Schematic diagram of train operation process

During the operating hours T of an URT line, there are one or more peaks and valleys in the passenger demand density curve at each station due to the differences in geographic locations and passenger carrying capacities [32]. As shown in Fig. 2(b), the whole day's operating hours T are divided into m peak hours, the time stamp of period T_m is in the range of $[t_m^s, t_m^e]$, and the passenger demand of station u during T_m is expressed as $\psi_{u,v}^{[t_m^s,t_m^e]}$.

According to the distribution characteristics of passenger demand density in each period T_m, based on the AFC data provided by the URT operator, using the uncertain lognormal distribution function to fit with the actual passenger flow distribution curve, the location scalar and scale scalar of the passenger flow demand at the station u in the mth period are set to be $\mu_{u,m}$ and $\sigma_{u,m}$ respectively, and the density of passenger demand $\varsigma_{u,v}(t)$ at station u in the period T_m is:

$$\varsigma_{u,v}(t)=\frac{1}{\sigma_{u,m}\sqrt{2\pi}t}\cdot\exp\left[-\frac{\left(\ln t-\mu_{u,m}\right)^2}{2\sigma_{u,m}^2}\right],\quad t\in[t_m^s,t_m^e] \tag{2}$$

According to Equation (2), the passenger demand $\psi_{u,v}^{[t_m^s,t_m^e]}$ of station u during T_m is calculated as follow:

$$\psi_{u,v}^{[t_m^s,t_m^e]}=\int_0^{t_m^e}\varsigma_{u,v}(t)\,\mathrm{d}t-\int_0^{t_m^s}\varsigma_{u,v}(t)\,\mathrm{d}t=\int_{t_m^s}^{t_m^e}\varsigma_{u,v}(t)\,\mathrm{d}t \tag{3}$$

To calculate the passenger demand during any period, it is defined $\psi_{u,v}^{[t_1,t_2]}$ to denote the passenger demand from station u to station v during $[t_1,t_2]$ where $t_1,t_2\in T$ and $t_1<t_2$. In the calculation of $\psi_{u,v}^{[t_1,t_2]}$, the distribution of t_1 and t_2 needs to be considered. As shown in Fig. 2(c), the calculation method of $\psi_{u,v}^{[t_1,t_2]}$ is shown in Equation (4) when $t_1,t_2\in T_m$:

$$\begin{aligned}\psi_{u,v}^{[t_1,t_2]}&=\int_0^{t_2}\varsigma_{u,v}(t)\,\mathrm{d}t-\int_0^{t_1}\varsigma_{u,v}(t)\,\mathrm{d}t=\int_{t_1}^{t_2}\varsigma_{u,v}(t)\,\mathrm{d}t\\&=\int_{t_1}^{t_2}\frac{1}{\sigma_{u,m}\sqrt{2\pi}t}\cdot\exp\left[-\frac{\left(\ln t-\mu_{u,m}\right)^2}{2\sigma_{u,m}^2}\right]\mathrm{d}t\end{aligned} \tag{4}$$

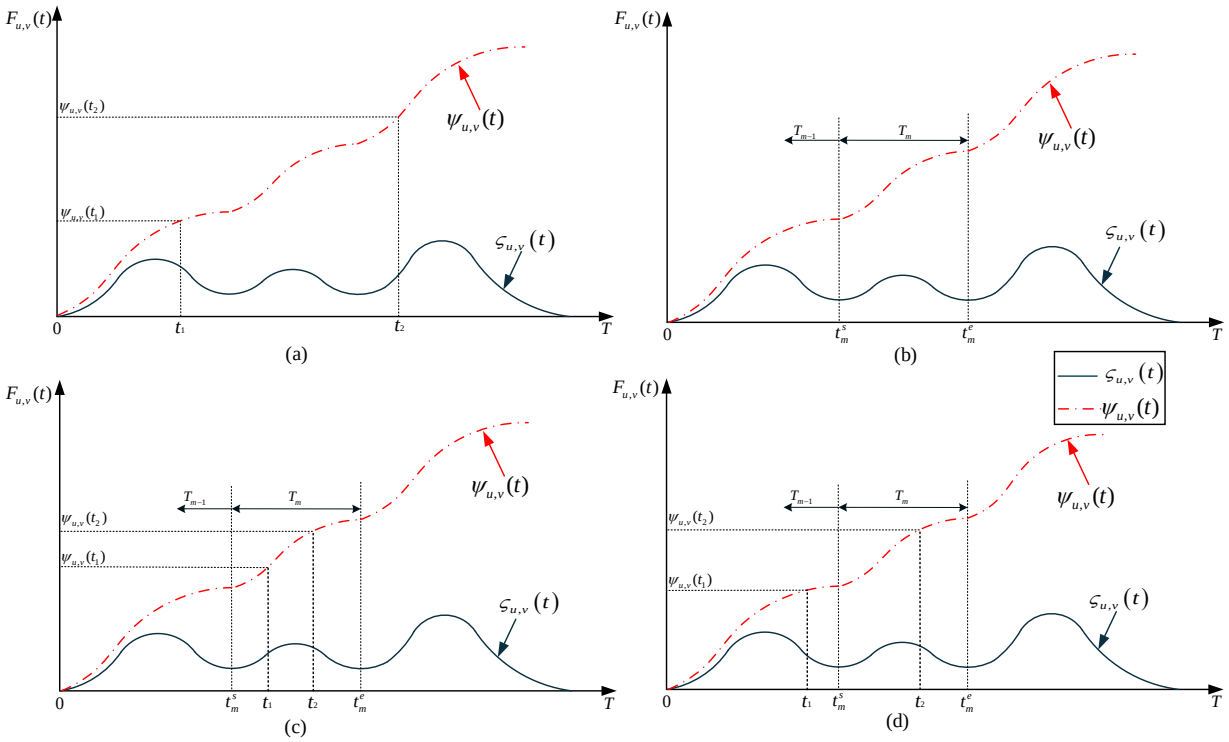

Fig. 2. Passenger demand in station u

Take $t_1 \in T_{m-1}, t_2 \in T_m$ in Fig. 2(d) as an example when t_1 and t_2 belonging to different peak periods. The calculation method of $\psi_{u,v}^{[t_1,t_2]}$ is shown in Equation (5):

$$\begin{aligned}\psi_{u,v}^{[t_1,t_2]} &= \int_{t_1}^{t_{m-1}^e} \varsigma_{u,v}(t)\,\mathrm{d}t + \int_{t_m^b}^{t_2} \varsigma_{u,v}(t)\,\mathrm{d}t \\ &= \int_{t_1}^{t_{m-1}^e} \frac{1}{\sigma_{u,m-1}\sqrt{2\pi t}} \cdot \exp\left[-\frac{\left(\ln t-\mu_{u,m-1}\right)^2}{2\sigma_{u,m-1}^2}\right]\mathrm{d}t \\ &+ \int_{t_m^b}^{t_2} \frac{1}{\sigma_{u,m}\sqrt{2\pi t}} \cdot \exp\left[-\frac{\left(\ln t-\mu_{u,m}\right)^2}{2\sigma_{u,m}^2}\right]\mathrm{d}t\end{aligned} \quad (5)$$

It should be noted that t_{m-1}^e and t_m^b are numerically equal due to the continuity between the period T_{m-1} and T_m. Based on Equations (4) and (5), the cumulative passenger demand $Q_u^{[t_1,t_2]}$ from station u during $[t_1,t_2]$ is given by:

$$Q_u^{[t_1,t_2]} = \sum_{v=u+1}^{|N|} \psi_{u,v}^{[t_1,t_2]},\ u,v \in \{1,2,\cdots,|N|\} \quad (6)$$

Similarly, the cumulative demand of passengers arriving at station v during $[t_1,t_2]$ can be defined as $P_v^{[t_1,t_2]}$ and calculated as follow:

$$P_v^{[t_1,t_2]} = \sum_{u=1}^{v-1} \psi_{u,v}^{[t_1,t_2]},\ u,v \in \{1,2,\cdots,|N|\} \quad (7)$$

C. Train operation strategy

In the established research literature on train operation scheme, most only consider scheduling trains of a single capacity type. In our study, we consider operating two different capacity trains on an URT corridor.

We first plot a single direction with four stations on an URT corridor and then design different train operation strategies to compare and analyze the total train operating costs of the strategies. In Fig. 3, we plot stations 1, 2, 3, and 4 in the same direction, determine the timestamp range [0,10], and set the physical distance between each neighboring station to equal 10. The red line represents the spatial and temporal trajectory of A-type train, which has a capacity of 100 and per unit length operation cost of 100. The green line represents the spatial and temporal trajectory of B-type train, a capacity of 150, per unit length operation cost of 200. The numbers in the white rectangles indicate the number of passengers on each train, and the numbers in the orange rectangles indicate the number of passengers who failed to board the train at each station.

The passenger demand is denoted by OD pairs, specifically 100 passengers from station 1 to station 4, 50 from station 2 to station 3, 100 from station 2 to station 4, and 50 from station 3 to station 4. Taking Fig. 3(a) as an example, all departing trains are A-type trains, and the timestamps of each train leaving station 1 are [1,3,5] and arriving at station 4 are [6,8,10], which means that the dwell time of each train is the same between adjacent stations and at each station, this means that each train has the same running time between neighboring stations and the same dwell time at each station, which is in line with the actual situation of the URT operation site. To fulfill the total passenger demand, it is necessary to organize the operation of three A-type trains, and the total operation cost F_1 is as follow:

$$F_1 = 100 \times (10+10+10) \times 3 = 9000 \quad (8)$$

In Fig. 3(a) after train 2 leaves station 2, the number of passengers in the cars reaches total capacity, but the number of unboarded passengers at station 2 is 50; similarly, when train 2 leaves station 3, also because the train is in total capacity resulting in the presence of unboarded passengers at station 3, to solve the phenomenon of stranding of passengers at stations 2 and 3, train 3 is operated to carry the unboarded passengers at stations 2 and 3.In Fig. 3(b), all B-type trains are dispatched to fulfill the pre-determined passenger travel demand, and the total operation cost F_2 is calculated as follows:

$$F_2 = 200 \times (10+10+10) \times 2 = 12000 \quad (9)$$

Although the number of trains operate is reduced, the operation cost of the B-train car is higher than that of the A-type train, resulting in F_2 is higher than F_1. We want to reduce the total operation cost while reducing the number of trains under the premise of fulfilling the passenger demand, so in Fig. 3(c), we organize the operation of A-type train as train 1 and B-type train as train 2. This operation strategy can also fulfill the task of carrying passengers, and the total operation cost F_3 is calculated as follow:

$$F_3 = 100 \times (10+10+10) + 200 \times (10+10+10) = 9000 \quad (10)$$

Compared to the operation strategy in Fig. 3(a), Fig. 3(c) does not increase the total operation cost but reduces the number of trains used and compared to Fig. 3(b), Fig. 3(c) reduces the total operation cost. Therefore, it is reasonable to use different types of trains to accomplish the task of carrying passengers, and next we will discover a mathematical model to optimize the train timetable, which in turn reduces the waiting time of passengers and total operation cost.

III. Mathematical Development

In this section, we use a modeling approach to specify the target problem into a mathematical model and optimize it. Due to the large number of factors affecting the optimization problem in the URT system, the following assumptions are made to highlight the focus of the problem considered in this paper:

Assumption 1: The operation time before the departure of the train at the originating station is not considered, the departure moment of the train at the originating station is regarded as the beginning of the train operation time.

Assumption 2: The interval distance between each station of the URT line is short, and the train running speed is lower, but the train start acceleration process is fast. We do not consider the additional time of the train starting and stopping at the station.

Assumption 3: On the URT line, the platforms of each station can meet the stopping conditions of different types of trains, and the different lengths of trains do not affect the process of boarding and alighting passengers.

Assumption 4: The stopping plan of the train is set as station stop mode, and the running time between each station and the dwell time at the station of each train are given in advance.

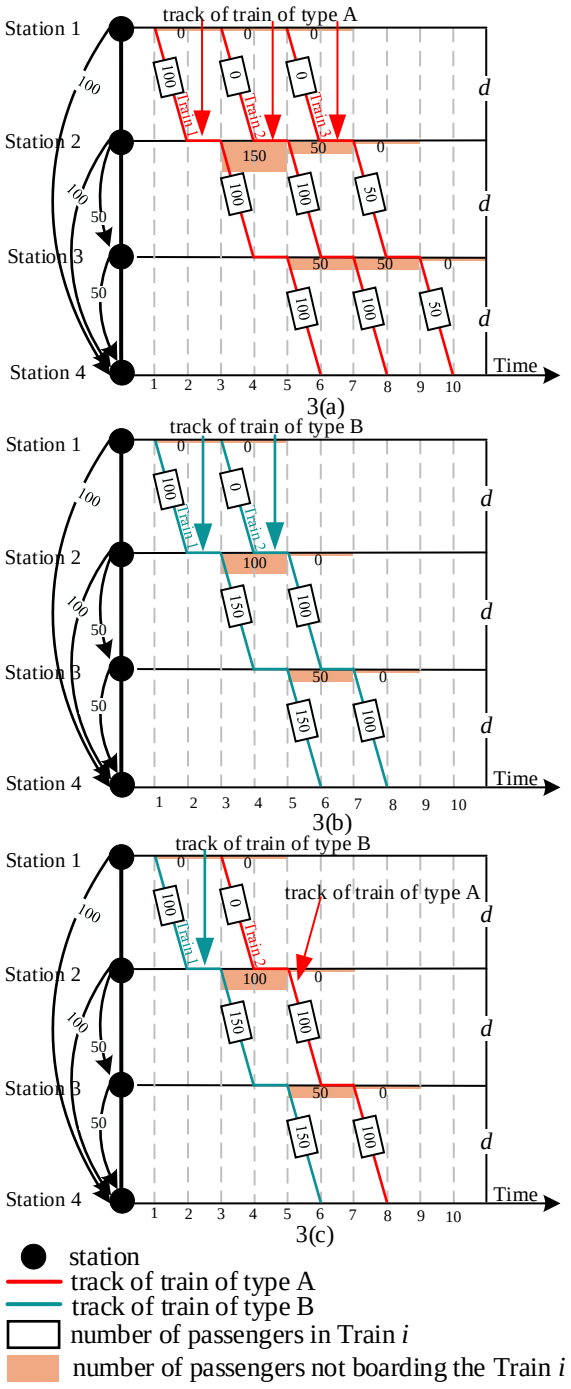

Fig. 3 Train operation modes with different capacities

A. Sets, Indexes and Parameters

To be able to visualize the mathematical model, Table. 1 lists the set, index and parameters used in Equations.

B. Variables

The objective of this study is to obtain a train timetable that minimizes total waiting time of passengers and total operating cost of the trains, but the fact that different trains have the same operation time $t_{n\text{-}1,n}$ between the same stations and the same dwell time at the same station makes the problem essentially transformed into determining the timestamp of departure of different types of trains at the originating station. Therefore, we design the decision variables $x_{i,k}$ and $y_{i,k}$ to denote the types of trains departing from the originating station in the upstream and downstream directions, respectively. For visualization, the variables in the model are listed and annotated in Table. 2.

Table. 1 Notations and definitions in the model

Notations	*Definitions*
Set	
T	Operation timestamp set of URT line
N	Stations set of URT line
$\overline{N}$	Set of upstream stations of URT line
$\underline{N}$	Set of downstream stations of URT line
K	Set of train types
I	Set of upstream trains in T
J	Set of downstream trains in T
Index	
t,t_1,t_2	Index of timestamp, $t,t_1,t_2 \in [0,T]$
k	Index of train type, $k \in K$
u,v,n	Index of station, $u,v,n \in N$
i,j	Index of train, $i \in I$, $j \in J$
Parameters	
A_k	Capacity of k-type train
c_k	unit operation cost of k-type train
$t^d_{i,n}, t^d_{j,n}$	dwell time at station n of upstream train i and downstream train j
$t_{n\text{-}1,n}$	operation time of trains between station n-1 and station n
t_e,t_l	timestamps for the start and end of T, $t_e,t_l \in T$
$h_{\max},h_{\min}$	maximum and minimum departure time between adjacent trains

Table. 2 Variables in the model

Auxiliary variables	
$\varsigma_{u,v}(t)$	passenger demand density from station u to station v at t
$\psi_{u,v}(t)$	passenger demand from station u to station v at t
$\psi_{u,v}^{[t_1,t_2]}$	passenger demand from station u to station v in time range $[t_1,t_2]$
$Q_n^{[t_1,t_2]}$	passenger demand departing from station n in time range $[t_1,t_2]$
$P_v^{[t_1,t_2]}$	passenger demand arriving at station v in time range $[t_1,t_2]$
$\alpha_{i,n},\alpha_{j,n}$	confidence level of the number of passengers boarding train i and train j
$\beta_{i,n},\beta_{j,n}$	confidence level of the number of passengers leaving train i and train j
$W_{i,n},W_{j,n}$	number of passengers waiting train i and train j at station n
$B_{i,n},B_{j,n}$	number of passengers boarding train i and train j at station n
$G_{i,n},G_{j,n}$	number of passengers leaving train i and train j at station n
$D_{i,n},D_{j,n}$	number of stranded passengers of train i and train j leaving station n
$C_{i,n},C_{j,n}$	number of passengers in the trains after train i and train j leave station n
$TW_{i,n},TW_{j,n}$	total waiting time of passengers at station n waiting for train i and train j
L_i^T, L_j^T	total operation distance of train i and train j in T
Decision variables	
$x_{i,k}$	0-1 binary variable; if train i chooses to use k -type train then $x_{i,k}$=1; otherwise $x_{i,k}$=0
$y_{i,k}$	0-1 binary variable; if train j chooses to use k -type train then $y_{i,k}$=1; otherwise $y_{i,k}$=0
$TA_{i,n},TA_{j,n}$	timestamp when train i and train j arrive at station n
$TD_{i,n},TD_{j,n}$	timestamp when train i and train j depart station n

C. Systemic constraints

In this section, we describe the constraints related to the safe realization of passenger operations of trains in URT

system, mainly from the aspects of safe train operation and passenger carrying capacity.

C. 1. Departure timestamp constraints:

$TD_{i,1}$ and $TD_{j,|N|+1}$ at which trains in different operation directions leave the originating station should be within the time range of the service provided by the URT line. $TD_{i,1}$ and $TD_{j,|N|+1}$ should be taken to satisfy Equations (11) and (12):

$$t_e \le TD_{i,1} \le t_l,\ i \in I \tag{11}$$

$$t_e \le TD_{j,|N|+1} \le t_l,\ j \in J \tag{12}$$

Typically, t_e and t_l of URT line are announced to passengers. The constraints in Equations (11) and (12) ensure that passengers arrive at the URT line in T then receive train service to fulfill their travel demand.

C. 2. Operation time constraints:

The above constraints only state the departure timestamp that need to be observed by trains leave the originating station and do not express the arrival and departure timestamp of trains at stations other than the originating station in detail. Combined with the premise of assumption 2, which disregard the additional time of train starting and stopping, Equations (13) and (14) are given to represent the arrival and departure timestamp of a train at each station, taking an upstream train as an example:

$$TA_{i,u+1} = TD_{i,u} + t_{u,u+1},\ i \in I,\ 1 \le u < |N| \tag{13}$$

$$TD_{i,u+1} = TA_{i,u+1} + t^d_{i,u+1},\ i \in I,\ 1 \le u < |N| \tag{14}$$

From Equation (13), it can be seen that the departure timestamp of train i from station u is added to the operation time $t_{u,u+1}$, and the result is when train i arrives at station u+1. Equation (14) describes the departure timestamp of train i from station u+1 with dwelling $t^d_{i,u+1}$ after arriving there. Similarly, Equations (15) and (16) express the operation constraints of the downstream trains:

$$TA_{j,u+1} = TD_{j,u} + t_{u,u+1},\ j \in J,\ |N|+1 \le u < 2|N| \tag{15}$$

$$TD_{j,u+1} = TA_{j,u+1} + t^d_{j,u+1},\ j \in J,\ |N|+1 \le u < 2|N| \tag{16}$$

C. 3. Departure interval constraints:

Since the dwell time of different trains at the same station and the operation time between stations are specified in advance, the most direct way to adjust train operation is to change the departure timestamp of trains from the originating station. Regardless of the upstream or downstream direction, adjacent trains in the same direction need to meet specific time intervals when leaving the originating station. The constraints on the departure time of adjacent trains from the originating station are as follows:

$$h_{\min} \le TD_{i+1,1} - TD_{i,1} \le h_{\max},\ i \in I \tag{17}$$

$$h_{\min} \le TD_{j+1,|N|+1} - TD_{j,|N|+1} \le h_{\max},\ j \in J \tag{18}$$

The operating company adjusts the departure intervals according to the passenger flow in different periods[13], but the departure intervals are within the specified values. Equations (17) and (18) based on $h_{\max}$ and $h_{\min}$ ensure that a safe operation distance is left between trains departing from the originating station.

C. 4. Train type constraints:

$$\sum_{k \in K} x_{i,k} = 1,\ i \in I \tag{19}$$

$$\sum_{k \in K} y_{j,k} = 1,\ j \in J \tag{20}$$

As shown in Equations (19) and (20), only one type of train could be used by train i or train j to provide service to passengers.

C. 5. Train capacity constraints:

URT operators stipulate that the number of passengers in the train when the train leaves stations does not exceed its authorized capacity, Equations (21) and (22) should be satisfied:

$$C_{i,u} \le \sum_{k \in K} A_k \cdot x_{i,k},\ i \in I,\ u \in \overline{N} \tag{21}$$

$$C_{j,u} \le \sum_{k \in K} A_k \cdot x_{j,k},\ j \in J,\ u \in \underline{N} \tag{22}$$

$C_{i,u}$ and $C_{j,u}$ are calculated according to the type of departing station u, divided into the originating station and the station other than the originating station. For example, in the upstream direction, the time interval $[TD_{i\text{-}1,u}, TD_{i,u}]$ between the departure of train i-1 and train i from station 1 is shown as the area shaded in green in Fig. 4. Passengers arriving at station 1 within the time interval $[TD_{i\text{-}1,u}, TD_{i,u}]$ can successfully board the train i. Without stranded passengers are at station1 after train i leaves, as shown in Fig. 4. Therefore, the number of passengers in the train after the train leaves the originating station is the number of passengers waiting at the station before the train arrives at the originating station, as shown in Equations (23) and (24):

$$C_{i,u} = W_{i,u},\ i \in I,\ u = 1 \tag{23}$$

$$C_{j,u} = W_{j,u},\ j \in J,\ u = |N|+1 \tag{24}$$

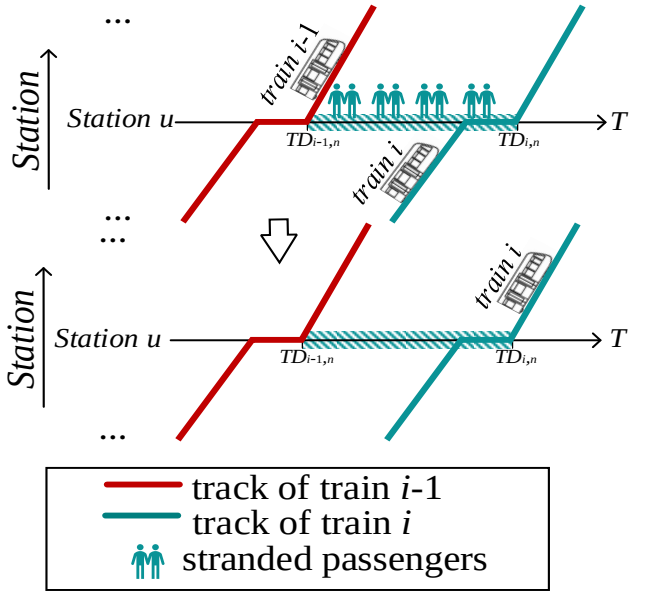

Fig. 4. Without stranded passengers

The differences in the travel purposes of passengers at each station on the URT line in T make the passenger demand random and fluctuating. The uncertainty of passenger demand is characterized by portraying the number of passengers waiting for trains at each station as an uncertain variable, and the uncertainty distribution function is used to express it. To ensure that the train schedule has strong robustness, the number of passengers waiting for trains at each station is expressed as the chance of being

satisfied at a specific confidence level using the idea of opportunity constraint. The confidence level constraints of $W_{i,u}$,$W_{j,u}$ in Equations (23) and (24) are expressed as follows:

$$M\left\{W_{i,u} \geq Q_u^{[TD_{i-1,u},TD_{i,u}]}\right\} \geq \alpha_{i,u},\ i \in I,\ u \in \overline{N} \quad (25)$$

$$M\left\{W_{j,u} \geq Q_u^{[TD_{j-1,u},TD_{j,u}]}\right\} \geq \alpha_{j,u},\ j \in J,\ u \in \underline{N} \quad (26)$$

$\alpha_{i,u}, \alpha_{j,u} \in (0,1)$ in Equations (23) and (24), $Q_u^{[TD_{i-1,u},TD_{i,u}]}$ and $Q_u^{[TD_{j-1,u},TD_{j,u}]}$ are calculated in Equation (6) in Section II. *B*.

Passenger boarding and alighting occurs upon arrival when a train travels between stations other than the originating station. When the train arrives at station u ($u \neq 1$ and $u \neq N+1$), passengers traveling to station u get off at this station, and passengers waiting for the train at the station can partially or fully board the train. The number of passengers in the train after the train departs from station u for different directions of operation is shown below:

$$C_{i,u} = C_{i,u-1} - G_{i,u} + B_{i,u},\ i \in I,\ 1 < u < |N| \quad (27)$$

$$C_{j,u} = C_{j,u-1} - G_{j,u} + B_{j,u},\ j \in J,\ |N|+1 < u < 2|N| \quad (28)$$

Equations (27) and (28) above denote the number of passengers who get off the train at station u after trains of different operation directions arrive, respectively. Similar to $W_{i,u}$ and $W_{j,u}$, the confidence level constraints are modeled using the chance programming method where $\beta_{i,u}, \beta_{j,u} \in (0,1)$, as follows:

$$M\left\{G_{i,u} \geq P_u^{[TA_{i,u},TA_{i+1,u}]}\right\} \geq \beta_{i,u},\ i \in I,\ u \in \overline{N} \quad (29)$$

$$M\left\{G_{j,u} \geq P_u^{[TA_{j,u},TA_{j+1,u}]}\right\} \geq \beta_{j,u},\ j \in J,\ u \in \underline{N} \quad (30)$$

In Equations (27) and (28), $B_{i,u}$ and $B_{j,u}$ are calculated as follows:

$$B_{i,u} = \sum_{k \in K} A_k \cdot x_{i,k} - C_{i,u-1} + G_{i,u},\ i \in I,\ 1 < u < |N| \quad (30)$$

$$B_{j,u} = \sum_{k \in K} A_k \cdot x_{j,k} - C_{j,u-1} + G_{j,u},\ j \in J,\ |N|+1 < u < 2|N| \quad (31)$$

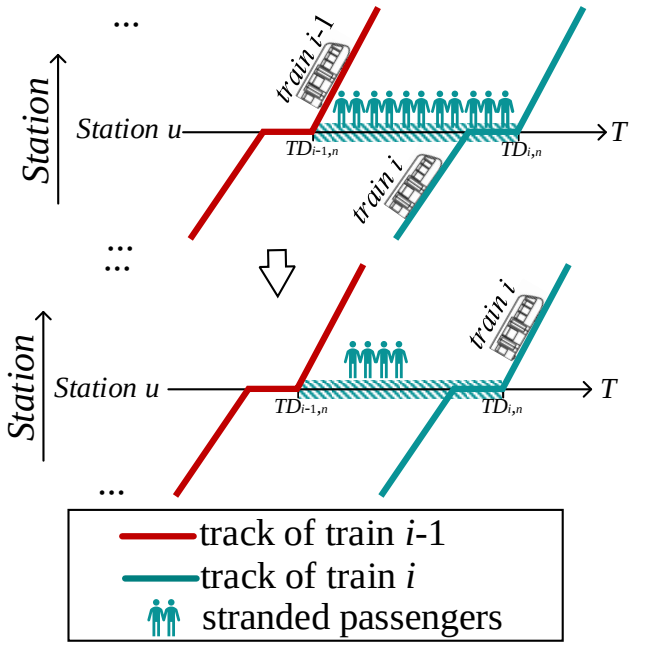

Fig. 5. Stranded passengers at stations n

It should not be overlooked that after the train has left station u, there may be stranded passengers at station u, as shown in Fig. 5, and some of the passengers who have not been able to board the train will continue to wait at station u for train i+1 or train j+1. The number of stranded passengers are calculated as follows:

$$D_{i,u} = W_{i,u} - B_{i,u},\ i \in I,\ 1 < u < |N| \quad (32)$$

$$D_{j,u} = W_{j,u} - B_{j,u},\ j \in J,\ |N|+1 < u < 2|N| \quad (33)$$

C. 6. Limitation of transportation capacity:

The transportation capacity provided by the trains operated by the URT operator shall meet the passenger flow demand of all stations on the line within T:

$$\sum_{i \in I} A_k \cdot x_{i,k} + \sum_{j \in J} A_k \cdot y_{j,k} \geq \sum_{n \in N} Q_n^{[0,T]},\ k \in K \quad (34)$$

D. Objective function

In this study, the optimization of train timetable on the URT line is considered from the perspectives of total waiting time (denoted by Z_1) and total operation cost (denoted by Z_2). The two optimization objectives (Z_1, Z_2) are described in the section.

D. 1. *Total waiting time*

Combining the operation of trains on the URT corridor with safety constraints, the total passenger waiting time for the entire line is calculated as follow:

$$Z_1 = \sum_{i \in I} \sum_{n \in \overline{N}} TW_{i,n} + \sum_{j \in J} \sum_{n \in \underline{N}} TW_{j,n} \quad (35)$$

The calculation of the total passenger waiting time on URT line is a summation of the passenger waiting times at each station in different operation directions. The optimal policy from the literature [33] is used to compute Equations (36):

$$TW_{i,n} = \begin{cases} 0.5 \cdot \left(TD_{i+1,n} - TA_{i,n}\right) \cdot W_{i,n}, \text{ when } D_{i,n} = 0, \\ 0.5 \cdot \left(TD_{i+1,n} - TA_{i,n}\right) \cdot W_{i,n} + t_n^{del}, \text{ otherwise,} \end{cases} i \in I,\ n \in \overline{N} \quad (36)$$

$$TW_{j,n} = \begin{cases} 0.5 \cdot \left(TD_{j+1,n} - TA_{j,n}\right) \cdot W_{j,n}, \text{ when } D_{i,n} = 0, \\ 0.5 \cdot \left(TD_{i+1,n} - TA_{i,n}\right) \cdot W_{i,n} + t_n^{del}, \text{ otherwise,} \end{cases} i \in I,\ n \in \underline{N} \quad (37)$$

When calculating t_n^{del}, take the passengers waiting for the upstream train i at station n as an example: when the phenomenon of passengers stranded occurs, the stranded passengers will continue to wait for the subsequent trains in the same direction to arrive at station n. Due to the passenger stranded phenomenon, there is a transfer effect, considering the same direction adjacent trains have standstill passengers, the calculation process of t_n^{del} is as follow:

$$t_n^{del} = \begin{cases} 0.5 D_{i+1,n} \left(TD_{i+1,n} - TA_{i,n}\right) \\ + D_{i,n} \left(TD_{i+1,n} - TA_{i,n}\right),\ i \in I,\ n \in \overline{N} \\ 0.5 D_{j+1,n} \left(TD_{j+1,n} - TA_{j,n}\right) \\ + D_{j,n} \left(TD_{j+1,n} - TA_{j,n}\right),\ j \in J,\ n \in \underline{N} \end{cases} \quad (38)$$

D.2. *Total operation cost*

The total operation cost at the end of T depends on the total distance operated by all trains during T. In this study, the operation cost of different types of trains for the same distance are different, Z_2 is calculated by considering both type of trains and distance of operation:

$$Z_2 = c_k\left(\sum_{i\in I}\sum_{k\in K} L_i^T x_{i,k} + \sum_{j\in J}\sum_{k\in K} L_j^T y_{j,k}\right) \tag{39}$$

E. Mathematical Model

According to the above constraints and objective functions, the optimization model of URT train timetable based on uncertain passenger flow is constructed as follows:

$$(\text{model})\begin{cases} z = (\min Z_1,\ \min Z_2) \\ s.t.\ \text{constraints}(11)\sim(33) \end{cases} \tag{40}$$

The above optimization model (41) is an uncertainty optimization model in which the confidence level constraints (Equations (25), (26), (29) and (30)) portray the chance that $W_{i,u}$ and $G_{i,u}$ can be satisfied by a certain confidence level. Although chance programming method can reflect the uncertainty of passenger demand, it increases the difficulty of model solving and computational analysis, so the confidence level constraint is replaced by a linear constraint combined with theorem 4.9 in the literature [34]. Since $Q_u^{[t_1,t_2]}, P_u^{[t_1,t_2]}\left(u\in N, t\in T\right)$ are uncertain variables obeying continuous distribution function, the uncertainty distribution function is $\varsigma_{u,v}(t), t\in[t_1,t_2]$, and the deterministic equivalent form of Equations (25), (26), (29) and (30) are as follows:

$$W_{i,u} \geq f_{Q_u^{[TD_{i-1,u},TD_{i,u}]}}(\alpha_{i,u}),\ i\in I,\ u\in \overline{N} \tag{41}$$

$$W_{j,u} \geq f_{Q_u^{[TD_{j-1,u},TD_{j,u}]}}(\alpha_{j,u}),\ j\in J,\ u\in \underline{N} \tag{42}$$

$$G_{i,u} \geq f_{P_u^{[TA_{i,u},TA_{i+1,u}]}}\left(\beta_{i,u}\right),\ i\in I,\ u\in \overline{N} \tag{43}$$

$$G_{j,u} \geq f_{P_u^{[TA_{j,u},TA_{j+1,u}]}}\left(\beta_{j,u}\right),\ j\in J,\ u\in \underline{N} \tag{44}$$

In the above Equations, $f_{Q_u^{[TD_{i-1,u},TD_{i,u}]}}(\alpha_{i,u}) = \varsigma^{-1}_{Q_u^{[TD_{i-1,u},TD_{i,u}]}}(\alpha_{i,u})$, $f_{Q_u^{[TD_{j-1,u},TD_{j,u}]}}(\alpha_{j,u}) = \varsigma^{-1}_{Q_u^{[TD_{j-1,u},TD_{j,u}]}}(\alpha_{j,u})$, $(i\in I\quad j\in J,\ u\in N)$ are the inverse uncertainty distributions function of $Q_u^{[TD_{i-1,u},TD_{i,u}]}, Q_u^{[TD_{j-1,u},TD_{j,u}]}$, $(i\in I, j\in J, u\in N)$. Similarly, the inverse uncertainty distribution function of $P_u^{[TD_{i-1,u},TD_{i,u}]}$, $P_u^{[TD_{j-1,u},TD_{j,u}]}$ $(i\in I, j\in J, u\in N)$ are $f_{P_u^{[TD_{i-1,u},TD_{i,u}]}}(\beta_{i,u}) = \varsigma^{-1}_{P_u^{[TD_{i-1,u},TD_{i,u}]}}(\beta_{i,u})$, $f_{P_u^{[TD_{j-1,u},TD_{j,u}]}}(\beta_{j,u}) = \varsigma^{-1}_{P_u^{[TD_{j-1,u},TD_{j,u}]}}(\beta_{j,u})$, $(i\in I,\ j\in J,\ u\in N)$.

After the above analysis, the model (46) is reconstructed based on (42)-(45) to transform the uncertainty optimization model into a deterministic optimization model:

$$(\text{model})\begin{cases} z = (\min Z_1,\ \min Z_2) \\ s.t.\ \text{constraints}(11)\sim(22),(25),(26) \\ \qquad\qquad (29)\sim(33),(39)\sim(42) \end{cases} \tag{45}$$

IV. Solution Approach

The calculation results of the above deterministic optimization model, which involves the departure moments of the trains at the originating station and considers the type of trains departed, is essentially a combination optimization problem, which can be solved using genetic algorithms (GA) [15]. Moreover, the spatial dimensions of each optimization objective of the established model are different, and it is necessary to consider using a multi-objective evolutionary algorithm to compute the nondominated solution of the model according to the constraints of each objective. NSGA-II has the advantages of fast operation speed and better convergence in solving the nondominated solution [36], is used as a baseline for the solving and is improved by combining with the Adaptive Large Neighborhood Search (ALNS) strategy.

A. Chromosome coding

The operating hours of URT line are discretized in minutes. A chromosome of length $|T|$ is designed, where each gene segment of the chromosome corresponds to the train departure type of the timestamp t. The corresponding codes take the values of 0,1 and 2, which indicate that no train, a low-capacity train, and a high-capacity train will be departed from originating station at timestamp t, respectively. As shown in Fig. 6, vector UT of a chromosome indicates the departure scheme at the upstream direction originating station; specifically, timestamp 1 runs a high-capacity train, and timestamp T runs a low-capacity train, and similarly in the vector UT of the chromosome, it indicates the departure scheme at the downstream direction originating station. The timestamp intervals of all adjacent trains from the originating station must be satisfied $h_{\min}$ and $h_{\max}$, each chromosome represents a feasible solution that satisfies all the constraints of the model (46).

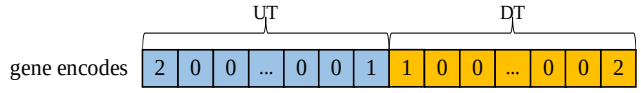

Fig. 6. Chromosome encoding design.

B. Crossover

Two chromosomes P_1 and P_2 are randomly selected in the population with crossover probability P_c. Two new chromosomes C_1 and C_2 are generated after crossover. The process of developing vector UT in chromosomes C_1 and C_2 is as follows:

Step 1: Before the crossover operation, vector UT in chromosomes P_1 and P_2 are randomly divided into d+1 segments according to the number of segmentation points d $(d\geq 1)$;

Step 2: Select the odd or even segments of vector UT in chromosomes P_1 and P_2 exchange them in equal parts to generate vector UT in chromosomes C_1 and C_2. The above crossover steps also apply to vector DT in chromosomes P_1 and P_2.

Fig. 7 shows the crossover process for selected chromosomes P_1 and P_2. when d=1 and even segments are exchanged equitably. Vector UT of chromosome P_1 is {1,0,0,0,2,…,0,1}, randomly divided into segments {1,0,0,0} and{2,…,0,1}. Vector UT of chromosome P_2 is also randomly divided into two segments, {2,0,0,0} and {1,0,0,1}. After crossover, vector UT in chromosome C_1 is {1,0,0,0,1,…,0,1}, and vector UT in chromosome C_2 is {2,0,0,0,2,…,0,1}; similarly, vector DT in chromosomes P_1 and P_2 form vector DT of chromosomes C_1 and C_2 after crossover. After the crossover operation, only the offspring

chromosomes that satisfy all constraints of model (46) are retained in the new population.

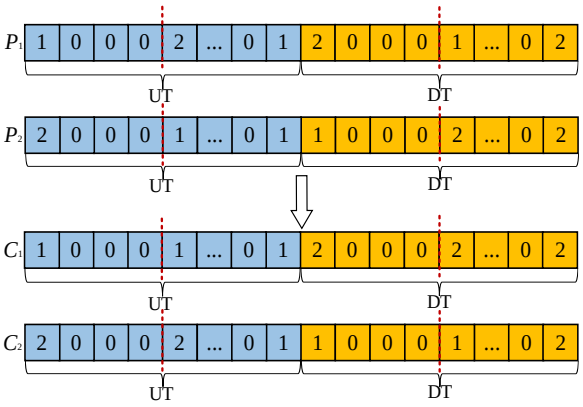

Fig. 7. Schematic diagram of the crossover process

C. Mutation

The process of generating a new chromosome by changing some of the gene values of a chromosome to other gene values with a certain probability is called mutation. Unlike paired chromosomes that undergo crossover operations to generate new offspring chromosomes, a single chromosome can generate a new chromosome by mutation. We combine ALNS strategy to design the mutation operator. Specifically, the process of chromosome mutation is divided into destroy and repair operation.

C. 1. Chromosome destroy operation

The objectives of the chromosome destroy operation are to increase the train full load rate, reduce the redundancy and total operation cost. These objectives can be achieved by reducing the number of trains operating or replacing high-capacity train with low-capacity train. Here, we design two different destroy strategies, and the detailed steps of the first destroy strategy are as follows:

Step 1: In the vector UT of chromosome, randomly select a timestamp t.

Step 2: Calculate the intervals between the departure timestamps of all adjacent trains ($TD_{i+1,1}$-$TD_{i,1}$) after timestamp t.

Step 3: Locate the minimal adjacent trains departure interval min ($TD_{i+1,1}$-$TD_{i,1}$) and reduce the gene value corresponding to the train departure timestamp $TD_{i,1}$ by one. At the same time, the same steps are performed in vector DT of chromosome, and the strategy is set to be executed a times in the destroy operation. The operation procedure of the first destroy strategy is shown in Fig. 8.

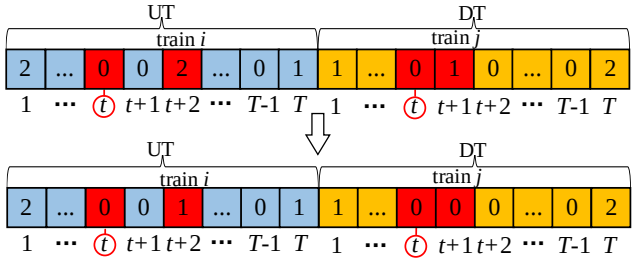

Fig. 8. Operation process of the first destroy strategy.

The detailed steps of the second destroy strategy are as follows:

Step 1: In vector UT of chromosome, choose a timestamp t randomly.

Step 2: Calculate the full load rate λ of all trains after timestamp t where $\lambda = \sum_{u=1}^{|N|} C_{i,u} / |N|$.

Step 3: Reduce the gene value by one corresponding to the departure timestamp $TD_{i,1}$ of the train with the smallest full load rate. At the same time, the same steps are performed in vector DT of chromosome, setting the strategy to be executed a times in the destroy operation.

C. 2. Chromosome repair operation

The goal of chromosome undergoing repair operation is to reduce total waiting time. This objective can be achieved by increasing the number of trains operating or replacing low-capacity train with high-capacity train. Here, we also design two different strategies for repair operation, the detailed steps of the first repair strategy are as follows:

Step 1: In vector UT of chromosome, choose a timestamp t randomly.

Step 2: Calculate the intervals between the departure timestamps of all adjacent trains ($TD_{i+1,1}$-$TD_{i,1}$) after timestamp t.

Step 3: Locate the maximum adjacent trains departure interval max ($TD_{i+1,1}$-$TD_{i,1}$) and add a high-capacity train between the departure timestamps of train i and train i+1. At the same time, the same steps are performed in vector DT of chromosome, and the strategy is set to be executed b times in the repair operation.

The detailed steps of the second repair strategy are as follows:

Step 1: In vector UT of chromosome, choose a timestamp t randomly.

Step 2: Calculate the full load rate λ of all trains after timestamp t.

Step 3: Locate departure timestamp $TD_{i,1}$ of the train i with the largest full load rate, and search backward for departure timestamp $TD_{i+1,1}$ of adjacent train i+1. Perform the following judgment after calculating $TD_{i+1,1}$-$TD_{i,1}$:

if $TD_{i+1,1}$-$TD_{i,1}$>$2I_{\min}$, add a high-capacity train between $TD_{i,1}$ and $TD_{i+1,1}$.

else, add a low-capacity train between $TD_{i,1}$ and $TD_{i+1,1}$.

During the chromosome mutation, the number of a and b for the execution of the destroy and repair operation strategies are decided according to the value of s. The calculations are shown in Equations (47) and (48):

$$s = 1 - \bar{\lambda} \tag{46}$$

$$\bar{\lambda} = \sum_{n \in N} Q_n^{[0,T]} / (\sum_{i \in I} A_{i,k} x_i + \sum_{j \in J} A_{j,k} y_j),\ k \in K \tag{47}$$

In the above Equations, $\bar{\lambda}$ represents the average full load rate of all trains. The smaller positive number s_0 is then taken for comparison with s:

If s>s_0, $\bar{\lambda}$ is lower, the number of chromosome destroy operation needs to be increased to reduce the train capacity redundancy; Else, $\bar{\lambda}$ is higher, the number of chromosome repair operation needs to be improved to reduce total waiting time.

D. Selection process

We copied the viable offspring chromosomes generated by crossover and mutation into a new population, performed fast non-dominated sorting simultaneously with the parent chromosomes, and used an elite retention strategy to obtain an optimized population.

V. Numerical Experiments

This section examines a real operational case study, which in turn evaluates the effectiveness of the developed model and the improved algorithm. The algorithms were coded in C. All numerical experiments were conducted on a computer with an Intel(R) Core (TM) i7-8750H @ 2.20 GHz CPU and 8.00 GB of RAM, with Microsoft Windows 10 (64-bit) as the operating system.

A. Set-up

Xi'an Metro Line 2 is a north-south URT corridor with a total length of 26.13 kms and 42 stations, the layout of which is shown in Fig. 9. The direction from Station 1 to Station 21 is defined as the upstream direction (Beiku-Weiquanan), and the direction from Station 22 to Station 42 is defined as the downstream direction (Weiquanan-Beiku).

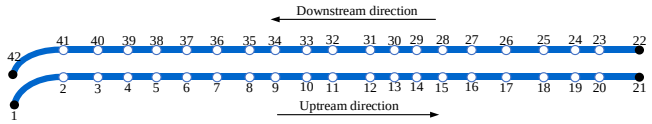

Fig. 9. Layout of the Xi'an metro line 2

Appendix A (Table. 8 and 9) gives primary data on train dwells and operates in both directions. h_{max} and h_{min} are 10min and 3min respectively, and the minimum turnaround time at both end turnback stations is 258 seconds. Low-capacity trains have a capacity of A_1=896, and high-capacity trains have a capacity of A_2=1376. The cost of operation for a low-capacity train is c_1=100CNY/km, and the cost of operation for a high-capacity train is c_2=200CNY/km.

B. Parameter selection

Setting reasonable parameters for the evolutionary algorithm used in the study directly affects its computational efficiency and reliability of the solution results[37], so we conducted experiments with different parameters under the numerical conditions in Table. 3. Under the needs of varying crossover probability ($P_c \in \{0.6,0.8\}$), mutation probability ($P_m \in \{0.2,0.4\}$), population size($N_p \in \{100,200\}$), and maximum number of iterations($I_m \in \{100,200\}$), the extreme and average values of each objective obtained are shown in Table. 4. When P_c=0.8, P_m=0.1, N_p=200 and I_m=200, the Pareto solution set obtained by solving contains the optimal values of each objective, so the above parameters are taken as fixed values. Meanwhile, using the simulation method in the literature [38], it is determined that $\alpha_{i,u}$=0.975, $\alpha_{j,u}$=0.964, $\beta_{i,u}$=0.971, $\beta_{j,u}$=0.967.

Table. 3 Selected pre-set parameters

s_0=0.15, d=5	$s>s_0$ a=*random* (30,50), b=*random* (20,30) $s \leq s_0$ b=*random* (30,50), a=*random* (20,30),

C. Comparison of results

In this section, we verify the practicality of the proposed method after analyzing the results. The AFC data of a particular day is extracted with a ime granularity of 30 minute. The passenger demand in different directions are shown in Fig. 10. To analyze the optimized train timetables, we introduce the actual train timetable on the corresponding dates of the passenger flow data for parameter comparison and then select the period with the most significant number of commuters and the most apparent congestion to the example, as shown in Fig. 11.

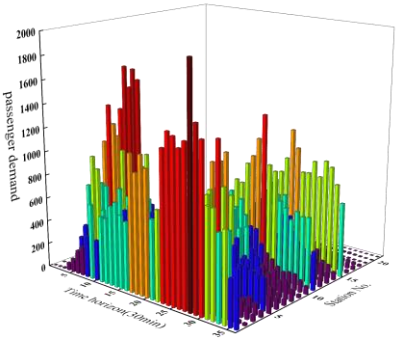

10(a) Upstream direction

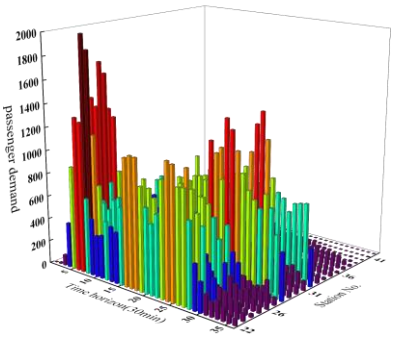

10(b) Downstream direction

Fig. 10. Schematic diagram of passenger demand

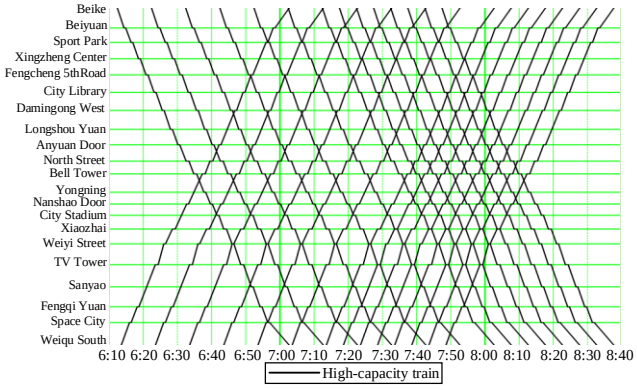

Fig. 11. Practical strategy from 6:10am to 7:55am

Specifically, 10-minute interval is observed between adjacent trains departing from station1 and station22 during 6:10am to 7:55am. With the further increase of passenger flow, the interval between adjacent trains departing from the originating station in the same direction is adjusted to 5 minutes after 7:15am.

Table. 4 Comparison of objective value with different parameters

P_c	P_m	N_p	I_m	min Z_1/minute		min Z_2/minute	
				Z_1	$\overline{Z_1}$	Z_2	$\overline{Z_2}$
0.6	0.1	100	100	1,759,284	2,637,254	1,418,638	1,592,929
0.6	0.1	100	200	1,703,661	2,431,497	1,406,078	1,591,985
0.6	0.1	200	100	1,742,349	2,524,134	1,519,884	1,601,223
0.6	0.1	200	200	1,713,583	2,327,825	1,401,919	1,596,753
0.6	0.05	100	100	1,844,219	2,839,648	1,572,570	1,600,632
0.6	0.05	100	200	1,793,182	2,782,152	1,528,942	1,596,464
0.6	0.05	200	100	1,697,867	2,386,429	1,576,696	1,587,791
0.6	0.05	200	200	1,671,879	2,274,147	1,469,011	1,492,348
0.8	0.1	100	100	1,729,239	2,347,213	1,477,946	1,635,157
0.8	0.1	100	200	1,724,467	2,317,439	1,467,226	1,611,281
0.8	0.1	200	100	1,671,584	2,217,214	1,475,373	1,643,893
0.8	0.1	200	200	1,652,987	2,157,897	1,398,124	1,513,345
0.8	0.05	100	100	1,783,271	2,345,914	1,427,309	1,522,010
0.8	0.05	100	200	1,693,737	2,276,341	1,416,182	1,491,328
0.8	0.05	200	100	1,723,548	2,571,848	1,434,270	1,592,762
0.8	0.05	200	200	1,672,145	2,431,297	1,426,826	1,609,998

The frequency of departures from upstream and downstream originating stations is 14 during 6:10am to 7:55am. Only a single high-capacity train is considered for scheduling during T. The departure frequency of both upstream and downstream directions is 146, Z_1=2321965min and Z_2=1525992CNY. Trains are organized in pairs during T. Implementing this type of operation plan is low, but achieving a high degree of coupling between trains and passenger demand is difficult.

To improve the coupling between trains and passenger flows, we use an improved algorithm to solve the designed model and obtain the Parete solution set. The black dots in Fig. 12 represent any of any Pareto solutions. After analyzing any of the Pareto solutions, the corresponding train timetable can be obtained. We choose three Pareto solutions (Pareto solutions 1,2, and 3 in Fig. 12) to evaluate the related train timetables after parsing them, where Pareto solution1 and 2 are two extreme solutions, and Pareto solution3 is non-polar solution.

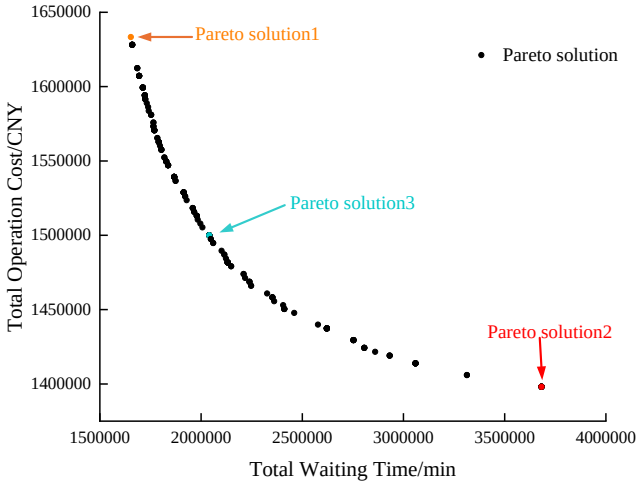

Fig. 12. Spatial distribution of Pareto solutions

After we parsed Pareto solutions 1,2 and 3, the results are shown in Table. 5. Pareto solution1 indicates that the total number of trains departures from originating station is 333 in T. Among them, there are 292 high-capacity trains and 41 low-capacity trains (the numbers in parentheses denote the number of low-capacity trains), which is comparable with the practical strategy; the total number of train timetables and Z_2 increased by 12.3% and 7.03% respectively, but Z_1 decreased by 28.8%. From the results, the train operating strategy corresponding to the Pareto solution1 effectively reduces the total passenger waiting time. However, it increases the number of trains and operation cost.

Table. 5 Comparison of results for different solution

Pareto solution	Number of trains in T		Z_1(min)	Z_2(CNY)
	Upstream	Downstream		
1	177(41)	156(0)	1,652,987	1,633,322
2	136(13)	138(0)	3,682,157	1,398,124
3	160(36)	145(0)	2,040,737	1,500,043

It should be noted that adjusting the train departure interval from a fixed interval to a non-fixed interval is the reason for increasing the number of trains in Pareto solution1. As shown in Fig. 13, the train timetable corresponding to Pareto solution 1 has 43 trains in all directions during 6:10am to 8:40am, and the departure intervals between adjacent trains are not limited to 5min and 10min. Therefore, expanding to T, adjusting the train departure interval to a non-fixed mode, it can increase the number of trains then improve the quality of passenger travel service.

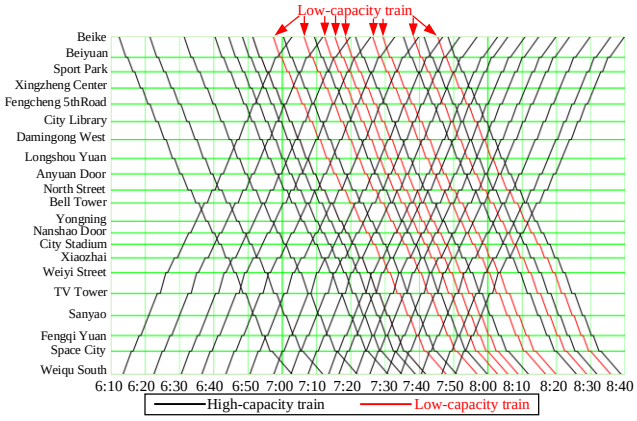

Fig. 13. Optimized solution 1 from 6:10am to 8:40am

After analyzing pareto solution2, we find that the total number of train departures is 274 during T, of which 261 are

high-capacity trains, and 13 are low-capacity trains, which reduces the number of high-capacity train by 10.6% compared to the practical strategy. In combination with using low-capacity trains to fulfill passengers demand, Z_2 reduces by 8.4%, but Z_1 increases by 58.6%.

Taking Fig. 14 as an example, the total number of trains scheduled in all directions only increased by three trains during 6:10am to 8:40am. Passenger demand showed a significant upstream trend after 6:50am, but four low-capacity trains are used after the moment. In the absence of a substantial increase in the total number of trains, the use of low-capacity trains reduces Z_2, but it results in a decrease in the ability of the trains to serve passengers. As a result, total number of train departures in all directions decreases by 6.16%, and 4.74% of high-capacity trains are replaced by low-capacity trains during T, thus leads to a significant increase of Z_1.

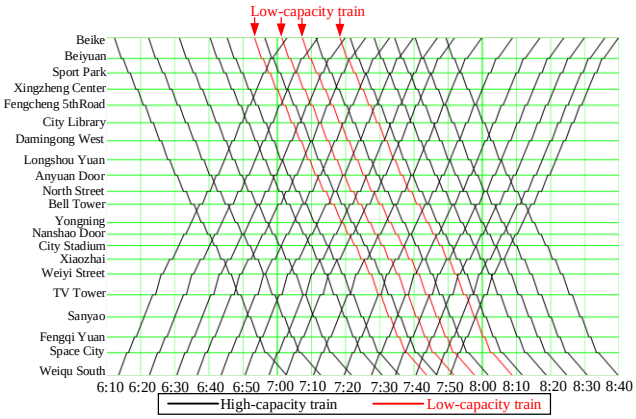

Fig. 14. Optimized solution 2 from 6:10am to 8:40am

After analyzing the Pareto solution3, we find that total number of train departures increased by 4.45% during T compared to the practical strategy, $Z_1$and Z_2 decrease by 12.1% and 1.7%, respectively. The number of low-capacity trains scheduled is 36 during T, it accounts for 11.8% of the total number of train departures.

As shown in Fig. 15, the number of low-capacity trains account for 24.4% of the total number of trains, and the total number of train departures in this period increased by 46.4% compared with Fig. 11. The number of train departures can be increased by adjusting the departure interval pattern of trains during T. Based on this, scheduling multiple types of trains can benefit traveling passengers and operators more than scheduling a single type of train.

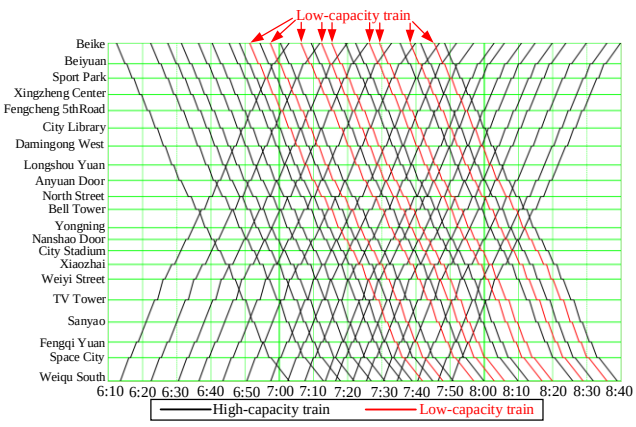

Fig. 15. Optimized solution 3 from 6:10am to 8:40am

From the above analysis, we draw the following conclusions:

(1) There is a conflict between the optimization objectives of the train timetable in this study, especially from the two extreme value solutions of Pareto solution1 and Pareto solution2; the solution that makes each objective optimal simultaneously does not exist.

(2) The decision maker can choose the train operation scheme according to the preference of different objectives. In Pareto solution2, although Z_2 is slightly reduced compared with the practical strategy, Z_1 is significantly increased. Therefore, the decision maker must make appropriate compromises between different optimization objectives when choosing the train operation scheme to avoid selecting the inferior solution under some criteria.

D. Algorithm effectiveness analysis

In this subsection, we use the parameter combinations (P_c=0.1, P_m=0.1, N_p=200, I_m=200) in section 5.2 to compare our improved algorithm with the standard NSGA-II algorithm regarding the quality of the solution set and computational speed. In section 4.3, we design two chromosome destroy and repair strategies, and it should be noted that the destroy and repair strategies are proposed to be interdependent, e.g., the first destroy strategy is used together with the first repair strategy, and the second destroy strategy is used together with the second repair strategy. For the convenience of presentation, as shown in Table 6, we name the algorithms according to the different destroy and repair strategies.

Table. 6 Nomenclature of algorithm under different mutation operations

Algorithm	Disruption Strategy	Repair strategy
NSGA-II	--	--
NSGA-II+B	1	1
NSGA-II+C	2	2
NSGA-II+D	1+2	1+2

Table. 7. shows the various types of metrics after solving the model (46) under different mutation conditions. We find that the quality and speed of the solutions of NSGA-II+B and NSGA-II+C are improved, which proves that the designed destroy and repair strategies are effective. The improvement is most apparent when all the destroy and repair strategies are used in NSGA-II+D at the same time.

Table. 7 Performance comparison of different algorithms

Algorithm	minZ_1	minZ_2	computational time(s)
NSGA-II	1,714,976	1,450,555	106.1
NSGA-II+B	1,694,829	1,433,515	101.4
NSGA-II+C	1,673,133	1,415,164	97.2
NSGA-II+D	1,652,987	1,398,124	91.7

VI. Conclusion

In this study, a bi-objective timetable optimization model considering scheduling different types of trains is developed under the condition of uncertain passenger demand in different directions of a subway line to reduce the total waiting time of passengers and the total operation cost of trains. We designed different ALNS strategies to obtain high-quality solutions during the chromosome mutation process. Subsequently, we implemented a numerical example with Xi'an Line 2 and verified the model's performance with

the improved algorithm by comparative analysis of the obtained solutions.

Our future research will focus on the following aspects. (1) In this paper, the uncertainty during train operation is not considered. Therefore, in our subsequent study, we extend the model to a robust optimization model based on considering the uncertainty of train running time. (2) In this study, the model was solved using a multi-objective heuristic algorithm, which easily falls into the dilemma of finding the optimal solution locally, so we will further explore the use of exact algorithms in this class of problems.

REFERENCES

[1] Xiao-ning Yang, and Jing Liu, "Sustainability in the evaluation of urban rail transit considering both firms and passengers perspectives: A dynamic network data envelopment analysis approach," Research in Transportation Business & Management, 51, 101071, 2023.

[2] Liu Yang, Koen H. Van Dam, Arnab Majumdar, Bani Anvari, Washington Y. Ochieng, and Lu-feng Zhang, "Integrated design of transport infrastructure and public spaces considering human behavior: A review of state-of-the-art methods and tools," Frontiers of Architectural Research, 8(4), 429-453, 2019.

[3] B. Szpigel, "Optimal train scheduling on a single track railway," Operations Research, 72: 343–352, 1973.

[4] Christian Liebchen, "The First Optimized Railway Timetable in Practice," Transportation Science, 42(4):420-435, 2008.

[5] Leiden Kroon, Gábor Maroti, and M. R. Helmrich, "Stochastic improvement of cyclic railway timetables," Transportation Research Part B Methodological, 42(6): 553-570, 2008.

[6] Leiden Kroon, Dennis Huisman, and Erwin Abbink, "The New Dutch Timetable: The OR Revolution," Interfaces, 39(1): 6-17, 2009.

[7] Bwo-Ren Ke, Chun-Liang Lin, and Hsien-Hung Chien, "Improvement of Freight Train Timetable for Single-Track Railway System,", 2012.

[8] Eva Barrena, David Canca, Leandro C. Coelho, and Gilbert Laporte, "Exact formulations and algorithm for the train timetabling problem with dynamic demand," Computers & Operations Research, 44(APR.):66-74, 2014.

[9] Si-Yu Zhuo, Jian-Rui Miao, Ling-Yuan Meng, Li-Ya Yang, and Pan Shang, "Demand-driven integrated train timetabling and rolling stock scheduling on urban rail transit line," Transportmetrica A: Transport Science, Vol.20, No.3 2324-9935, 2023.

[10] Li-Xing Yang, Ke-Ping Li, and Zi-You Gao, "Train Timetable Problem on a Single-Line Railway with Fuzzy Passenger Demand," IEEE Transactions on Fuzzy Systems, 17(3):617-629, 2009.

[11] Bucak Serkan, and Demirel Tufan, "Train timetabling for a double-track urban rail transit line under dynamic passenger demand," Computers & Industrial Engineering, 16, 2022.

[12] Jie Liu, David Canca, and Hong-Xia Lv, "Spatiotemporal synchronous coupling algorithm for urban rail transit timetables design under dynamic passenger demand," Applied Mathematical Modelling, 119, 239-256, 2023.

[13] Ling-Yun Meng, and Xue-Song Zhou, "An integrated train service plan optimization model with variable demand: A team-based scheduling approach with dual cost information in a layered network," Transportation Research Part B: Methodological, 125(JUL.): 1-28, 2019.

[14] Cong-Cong Gong, Jun-Gang Shi, Yan-Hui Wang, Hou-Sheng Zhou, Li-Xing Yang, De-Wang Chen, and Han-Chuan Pan, "Train timetabling with dynamic and random passenger demand: A stochastic optimization method," Transportation Research Part C: Emerging Technologies, 123, 102963, 2021.

[15] Hui-Ming Niu, and Xue-Song Zhou, "Optimizing urban rail timetable under time-dependent demand and oversaturated conditions," Transportation Research Part C, 36:212-230, 2013.

[16] Hui-Ming Niu, Xue-Song Zhou, and Ru-Hu Gao, "Train scheduling for minimizing passenger waiting time with time-dependent demand and skip-stop patterns: Nonlinear integer programming models with linear constraints," Transportation Research Part B, 76 (Jun.): 117-135, 2015.

[17] Peng-Li Mo, Li-Xing Yang, Andrea D'Ariano, Jia-Teng Yin, Yu Yao, and Zi-You Gao, "Energy-Efficient Train Scheduling and Rolling Stock Circulation Planning in a Metro Line: A Linear Programming Approach," IEEE Transactions on Intelligent Transportation Systems, 21(9):3621-3633, 2020.

[18] Jia-Wei Yuan, Yuan Gao, Shu-Kai Li, Pei Liu, and Li-Xing Yang, "Integrated optimization of train timetable, rolling stock assignment and short-turning strategy for a metro line," European Journal of Operational Research, (3):301, 2022.

[19] Xiao-Peng Tian, and Hui-Ming Niu, "A bi-objective model with sequential search algorithm for optimizing network-wide train timetables," Computers & Industrial Engineering, 127, 1259-1272, 2019.

[20] Xiao-Peng Tian, and Hui-Ming Niu, "Optimization of demand-oriented train timetables under overtaking operations: A surrogate-dual-variable column generation for eliminating indivisibility," Transportation Research Part B: Methodological, 142, 143-173, 2020.

[21] Xin Yang, Xiang Li, Bin Ning, and Tao Tang, "A Survey on Energy-Efficient Train Operation for Urban Rail Transit," IEEE transactions on intelligent transportation systems, (1):17, 2016.

[22] Xiang Li, De-Chun Wang, Ke-Ping Li, and Zi-You Gao, "A green train scheduling model and fuzzy multi-objective optimization algorithm," Applied Mathematical Modelling, 37(4):2063-2013, 2013.

[23] Li-Jun Sun, Jian-Gang Jin, Der-Horng Lee, Kay W. Axhausen, and Alexander Erath, "Demand-driven timetable design for metro services," Transportation Research Part C: Emerging Technologies, 46, 284-299, 2014.

[24] Hamed Pouryousef, Pasi Lautala, and David Watkins, "Development of hybrid optimization of train schedules model for N-track rail corridors," Transportation Research Part C: Emerging Technologies, 67, 169-192, 2016.

[25] David Canca, Alejandro Zarzo, Algaba Encarnación, and Eva Barrena, "Confrontation of Different Objectives in the determination of train scheduling," Procedia - Social and Behavioral Sciences, 20:302-312, 2011.

[26] J. E. Cury, F. A. C. Gomide, and M. J. Mendes, "A methodology for generation of optimal schedules for an underground railway system," IEEE Transactions on Automatic Control, 25(2):217-222, 1979.

[27] Thomas Albrecht, "Automated timetable design for demand-oriented service on suburban railways," Public Transport, 1(1):5-20, 2009.

[28] Hui-Jun Sun, Jian-Jun Wu, Hong-Nan Ma, Xin Yang and Zi-You Gao, "A Bi-Objective Timetable Optimization Model for Urban Rail Transit Based on the Time-Dependent Passenger Volume," IEEE Transactions on Intelligent Transportation Systems, 2018.

[29] Xin Yang, Bin Ning, Xiang Li and Tao Tang, "A Two-Objective Timetable Optimization Model in Subway Systems," IEEE Transactions on Intelligent Transportation Systems, 15, 5, 1913-1921, 2014.

[30] Peng-Li Mo, Li-Xing Yang, Yan-Hui Wang, and Jian-Guo Qi, "A flexible metro train scheduling approach to minimize energy cost and passenger waiting time," Computers & Industrial Engineering, 132(JUN.):412-432, 2019.

[31] Li-Xing Yang, Jian-Guo Qi, Shu-Kai Li, and Yuan Gao, "Collaborative optimization for train scheduling and train stop planning on high-speed railways," Omega: The International Journal of Management Science, 64(Oct.):57-76, 2016.

[32] David Canca, Eva Barrena, Encarnación Algaba, and Alejandro Zarzo, "Design and analysis of demand-adapted railway timetables," Journal of Advanced Transportation, 48(2):119–137, 2014.

[33] Heniz Spiess, and Michael Florian, "Optimal strategies: A new assignment model for transit networks," Transportation Research Part B: Methodological, 23(2):83-102, 2008.

[34] Bao-Ding Liu, "Uncertainty theory". 2nd ed[M]. 2007.

[35] Feng Niu, Jian-Guo Qi and Jin Qin, "Optimization Model for Train Stopping Plan on High-speed Railway Corridor with Uncertain Passenger Demands," Journal of the China Railway Society, 38(07):1-7, 2016.

[36] Chih-Hao Lin, and Pei-Ling Lin, "Improving the non-dominated sorting genetic algorithm using a gene-therapy method for multi-objective optimization," Journal of Computational Science, 5(2):170-183, 2014.

[37] A. E. Eiben, and S. K. Smit, "Parameter tuning for configuring and analyzing evolutionary algorithms," Swarm & Evolutionary Computation, 1(1):19–31, 2011.

[38] Run-Yu Wu, Cun-Jie Dai, Xiao-Quan Wang, and Shi-Xiang Wan, "Simulation and Optimization of Intelligent Evacuation System for Urban Rail Transit Station," Engineering Letters, 31(4), 1919-1927, 2023.

Runyu Wu was born in Gansu, China, in 2000. He is a postgraduate student at School of Traffic and Transportation, Lanzhou Jiaotong University, China, majoring in transportation planning and management. He has a strong interest in computer simulation theory of rail transit and transportation organization of urban rail transit.

APPENDIX I

Table. 8 Train dwell time of Xi'an metro line 2

Station	Dwelling Time(s)	
	Upstream	Downstream
Beike	140	140
Beiyuan	30	32
Sports Park	30	32
Xingzheng Center	32	30
Fengcheng 5thRoad	35	32
City Library	35	32
Damingong West	34	30
Longshou Yuan	35	35
Anyuan Door	32	35
North Street	50	50
Bell Tower	50	50
Yongning	32	30
Nanshao Door	34	32
TV Tower	50	50
Sanyao	32	32
Fengqi Yuan	34	30
Space City	34	30
Weiqu South	210	210
City Stadium	34	32
Xiaozhai	50	50
Weiyi Street	34	30

Table. 9 Train operation time of xi'an metro line 2

Segment	Running time(s)
Beike-Beiyuan	122
Beiyuan-Sports Park	94
Sports Park-Xingzheng Center	100
Xingzheng Center-Fengcheng 5thRoad	100
Xingzheng Center-City Library	107
City Library-Damingong West	110
Damingong West-Longshou Yuan	111
LongshouYuan-Anyuan Door	98
Anyuan Door-North Street	111
North Street-Bell Tower	85
Bell Tower-Yongning	128
Yongning-Nanshao Door	82
Nanshao Door-City Stadium	79
City Stadium-Xiaozhai	86
Xiaozhai-Weiyi Street	95
Weiyi Street-TV Tower	120
TV Tower-Sanyao	136
Sanyao-Fengqi Yuan	122
Fengqi Yuan-Space City	100
Space City-Weiqu South	144
Weiqu South-Space City	142
Space City-Fengqi Yuan	98
Fengqi Yuan-Sanyao	120
Sanyao-TV Tower	140
TV Tower-Weiyi Street	115
Weiyi Street- Xiaozhai	98
Xiaozhai City-Stadium	90
City Stadium-Nanshao Door	75
Nanshao Door-Yongning	85
Yongning-Bell Tower	130
Bell Tower-North Street	85
North Street-Anyuan Door	110
Anyuan Door-LongshouYuan	103
Longshou Yuan-Damingong West	108
Damingong West-City Library	105
City Library- Fengcheng 5thRoad	112
Fengcheng5thRoad-XingzhengCenter	100
Xingzheng Center-Sports Park	102
Sports Park-Beiyuan	98
Beiyuan-Beike	120